

Bph6 encodes an exocyst-localized protein and confers broad resistance to planthoppers in rice

Jianping Guo¹, Chunxue Xu¹, Di Wu¹, Yan Zhao¹, Yongfu Qiu¹, Xiaoxiao Wang¹, Yidan Ouyang², Baodong Cai³, Xin Liu⁴, Shengli Jing¹, Xinxin Shangguan¹, Huiying Wang¹, Yinhua Ma¹, Liang Hu¹, Yan Wu¹, Shaojie Shi¹, Wenliang Wang¹, Lili Zhu¹, Xun Xu⁴, Rongzhi Chen¹, Yuqi Feng³, Bo Du^{1*} and Guangcun He^{1*}

The brown planthopper (BPH) and white-backed planthopper (WBPH) are the most destructive insect pests of rice, and they pose serious threats to rice production throughout Asia. Thus, there are urgent needs to identify resistance-conferring genes and to breed planthopper-resistant rice varieties. Here we report the map-based cloning and functional analysis of *Bph6*, a gene that confers resistance to planthoppers in rice. *Bph6* encodes a previously uncharacterized protein that localizes to exocysts and interacts with the exocyst subunit OsEXO70E1. *Bph6* expression increases exocytosis and participates in cell wall maintenance and reinforcement. A coordinated cytokinin, salicylic acid and jasmonic acid signaling pathway is activated in *Bph6*-carrying plants, which display broad resistance to all tested BPH biotypes and to WBPH without sacrificing yield, as these plants were found to maintain a high level of performance in a field that was heavily infested with BPH. Our results suggest that a superior resistance gene that evolved long ago in a region where planthoppers are found year round could be very valuable for controlling agricultural insect pests.

Cultivated rice (*Oryza sativa* L.) grows under a wide range of environmental conditions; however, most rice is cultivated in irrigated or rain-fed fields, which provide warm, humid environments that promote the proliferation of insects. Hundreds of insect species reportedly feed on rice¹, but the brown planthopper (*Nilaparvata lugens* Stål; hereafter referred to as BPH) and the white-backed planthopper (*Sogatella furcifera* Horvath; hereafter referred to as WBPH) are the most destructive. Planthoppers cause direct damage by sucking sap from the phloem of susceptible rice varieties, resulting in ‘hopperburn’, which is characterized by extensive wilting, yellowing and lethal drying of rice². Planthoppers may also indirectly damage rice plants by transmitting viral disease agents^{2,3}. The BPH is believed to have undergone a host shift from *Leersia* to *Oryza* in tropical Asia about 0.25 million years ago⁴. These migratory pests remain active year round in warm tropical areas and can travel thousands of kilometers over land and sea, which poses serious threats to annual global rice production^{2,5,6}. In recent decades the abundance and severity of planthopper infestations have increased. Because the planthoppers have developed resistance to insecticides that were previously effective for controlling them⁷, there is a clear need to exploit planthopper-resistance genes for breeding resistant cultivars.

Planthopper resistance in rice was first reported in the variety Mudgo in 1969^{8,9}. It involves either antixenotic mechanisms that repel the insects or antibiotic mechanisms that harm the insects and reduce their survival, growth or reproduction rates. On the basis of rice resistance scores and/or planthopper insect performance, a number of planthopper-resistance genes have been detected in cultivated and wild rice species^{4,10}. Several BPH-resistance genes (*Bph14*, *Bph26*, *Bph3*, *Bph29*, *Bph9* and *Bph32*)

have previously been cloned^{11–17}, just one of which (*Bph3*) confers broad-spectrum resistance to BPH and WBPH¹⁴. Thus, there are still urgent needs to identify new types of resistance genes and elucidate resistance mechanisms.

Results

Map-based cloning of *Bph6*. The Bangladesh landrace Swarnalata carries a dominant BPH resistance gene, *Bph6*¹⁸, which was previously mapped to the long arm of chromosome 4 between the SSR (simple sequence repeat) markers Y19 and Y9¹⁹. In the present study, we have performed high-resolution mapping using 4,300 BC₃F₂ plants derived by crossing Swarnalata with 9311 (recurrent parent)¹⁹ to further narrow the candidate region between the H and Y9 markers (Fig. 1a). We sequenced this fragment (18.1 kb) in Swarnalata (Fig. 1a) and found two predicted genes in it, which we designated *Gene1* and *Gene2* (Fig. 1b). We obtained full-length cDNAs that corresponded to both genes. We observed that there were many differences in the deduced amino acid sequences encoded by *Gene1* in Swarnalata and Nipponbare, but there was 100% identity in the amino acid sequences encoded by *Gene2* for both landraces (Supplementary Fig. 1). To test which gene was *Bph6*, we transformed the candidate *Gene1* or *Gene2* into the BPH-susceptible rice Nipponbare. In complementation tests, segregation of resistance was detected in all 28 independent T₁ progenies of the lines that were transgenic for *Gene1* (Supplementary Table 1 and Supplementary Fig. 2). Further checks with the T₂ progenies from two T₁ single-copy *Gene1*-transgenic lines showed that BPH resistance scores cosegregated with the transgene and that the segregation of the resistant, segregating and susceptible plants was in agreement with a 1:2:1 ratio (Supplementary Fig. 3). Furthermore, T₂ families with

¹State Key Laboratory of Hybrid Rice, College of Life Sciences, Wuhan University, Wuhan, China. ²National Key Laboratory of Crop Genetic Improvement, Huazhong Agricultural University, Wuhan, China. ³Key Laboratory of Analytical Chemistry for Biology and Medicine (Ministry of Education), College of Chemistry and Molecular Sciences, Wuhan University, Wuhan, China. ⁴BGI-Shenzhen, Shenzhen, China. Jianping Guo, Chunxue Xu and Di Wu contributed equally to this work. *e-mail: boddu@whu.edu.cn; gche@whu.edu.cn

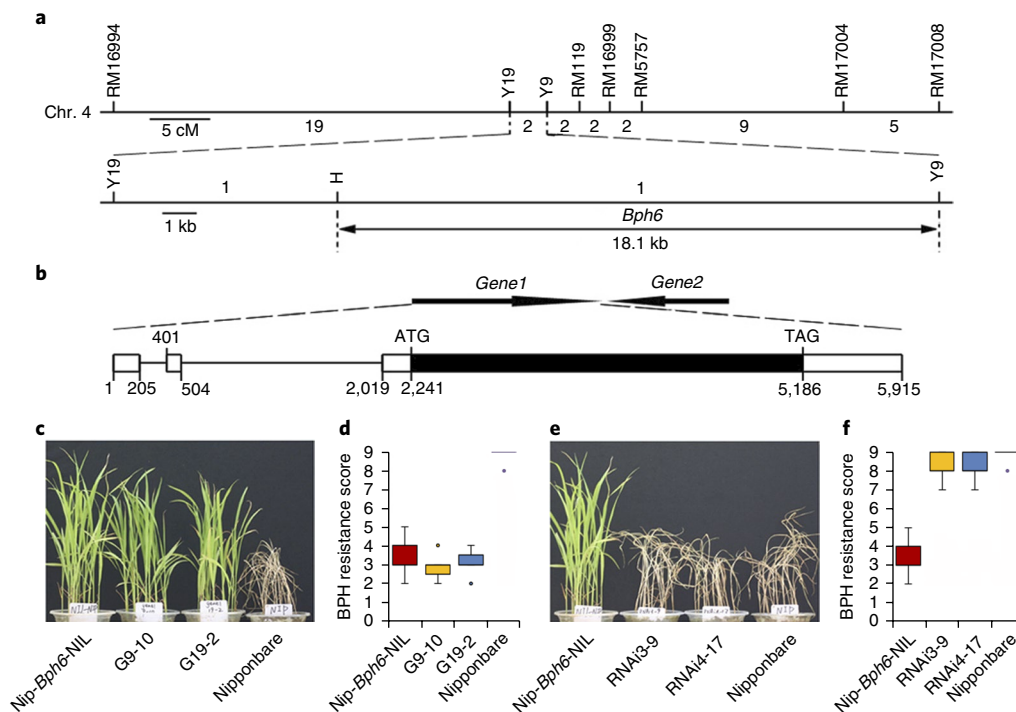


Fig. 1 | Map-based cloning of *Bph6*. **a**, Fine mapping of *Bph6* to an 18.1-kb genomic region, which contains two predicted genes. Numbers under the linkage map indicate numbers of recombinants detected between the molecular markers. **b**, Structure of *Bph6*. White boxes represent the 5' and 3' UTRs, the black box represents the coding sequence, and the thin line represents the intron. ATG and TAG indicate the start and stop codons of the ORF. The position (in base pairs) starting at the first nucleotide in the transcript was determined by RACE. **c**, Photograph of representative *Bph6*-transgenic seedlings that were damaged by BPH. **d**, BPH-resistance scores of the *Bph6*-transgenic lines. G9-10 and G19-2 are homozygous T_2 progeny from independent *Bph6* complementation transformants. **e**, Photograph of representative *Bph6*-RNAi seedlings damaged by BPH. **f**, BPH-resistance scores of the *Bph6*-RNAi lines. RNAi3-9 and RNAi4-17, homozygous T_2 progeny plants of independent *Bph6*-RNAi transformants suppressing *Bph6* in Nip-*Bph6*-NIL plants. In **d** and **f**, the lower scores indicate higher resistance to the insect, and the higher scores indicate higher susceptibility to BPH; data were collected 7 d after BPH infestation ($n=3$ independent experiments, with each pooled with 15 individual plants). In the box plots, the center value is the median, and the bottom and top edges of the boxes indicate the 25th and 75th percentiles; whiskers mark the range of the data, excluding outliers.

homozygous *Gene1* showed high resistance and survived under BPH infestation, whereas wild-type plants were killed within 7 d of BPH infestation (Fig. 1c,d). In stark contrast, *Gene2*-transgenic lines were susceptible (like the wild-type plants) and killed within 7 d; thus, *Gene2* is unlikely to be a BPH resistance gene (Supplementary Fig. 2). We also conducted confirmatory gene-silencing tests. We have previously developed near-isogenic lines (NILs) carrying *Bph6* in the 9311 and Nipponbare backgrounds¹⁹ (respectively named 9311-*Bph6*-NIL and Nip-*Bph6*-NIL here), which showed high resistance to BPH infestation (Supplementary Fig. 4). We transformed the Nip-*Bph6*-NIL with an RNA interference (RNAi) construct targeting *Gene1*. Segregation of resistance was detected in all eight independent T_1 progenies of the *Gene1*-specific RNAi-transgenic lines (Supplementary Table 1), and further checks with T_2 progenies from two T_1 single-copy transgenic lines showed that BPH resistance scores cosegregated with the transgene and that the segregation of the resistant, segregating and susceptible plants was in agreement with a 1:2:1 ratio (Supplementary Fig. 3). Expression of *Gene1* was suppressed in the RNAi lines (Supplementary Fig. 5), which were susceptible and killed by BPH insects (Fig. 1e,f). These observations demonstrate that *Gene1* (NCBI accession KX818197) is the BPH-resistance-conferring gene *Bph6*.

***Bph6* encodes a previously uncharacterized protein that is localized to the exocyst.** *Bph6* was predicted to encode a protein of 981 amino acids (Supplementary Fig. 2a) that has no similarity to any known proteins. To determine its subcellular localization, we

coexpressed BPH6-GFP or BPH6-YFP with organelle marker proteins in rice protoplasts. The fluorescent BPH6 signals did not colocalize with any of the standard organelle markers for the endoplasmic reticulum (ER), cis-Golgi apparatus, trans-Golgi network/early endosomes (TGN/EE), tonoplast and nucleus (Supplementary Fig. 6). However, we observed clear colocalization of BPH6 and its allelic proteins in Nipponbare and 9311 with EXO70E2, an exocyst complex subunit²⁰ (Fig. 2a). We also coexpressed the genes encoding other exocyst subunits, *Exo84b* and *Sec10*, with *Bph6* in rice protoplasts. Confocal microscopy showed that BPH6 colocalized with these exocyst subunits (Fig. 2a). These results strongly indicate that BPH6 protein localizes with the exocyst complex.

We also assessed the *Bph6* expression pattern by RNA in situ hybridization. The signals indicated that *Bph6* and its allele in Nipponbare were strongly expressed in sclerenchyma tissues, vascular bundles and companion cells in the leaf sheaths and leaves of rice plants (Fig. 2b–e and Supplementary Fig. 7). Real-time RT-PCR analysis showed that *Bph6* was expressed in the radicle, plumule, leaf blade, leaf sheath, stem, young panicle and endosperm (Fig. 2f). The transcript levels did not significantly differ between Nip-*Bph6*-NIL and Nipponbare plants in leaf sheath and stem tissues, which BPH often infested. Furthermore, *Bph6* expression was not significantly upregulated at either the transcript or protein level by BPH feeding (Fig. 2g and Supplementary Fig. 8).

BPH6 interacts with OsEXO70E1 and promotes exocytosis. The plant exocyst has recently emerged as an important battleground

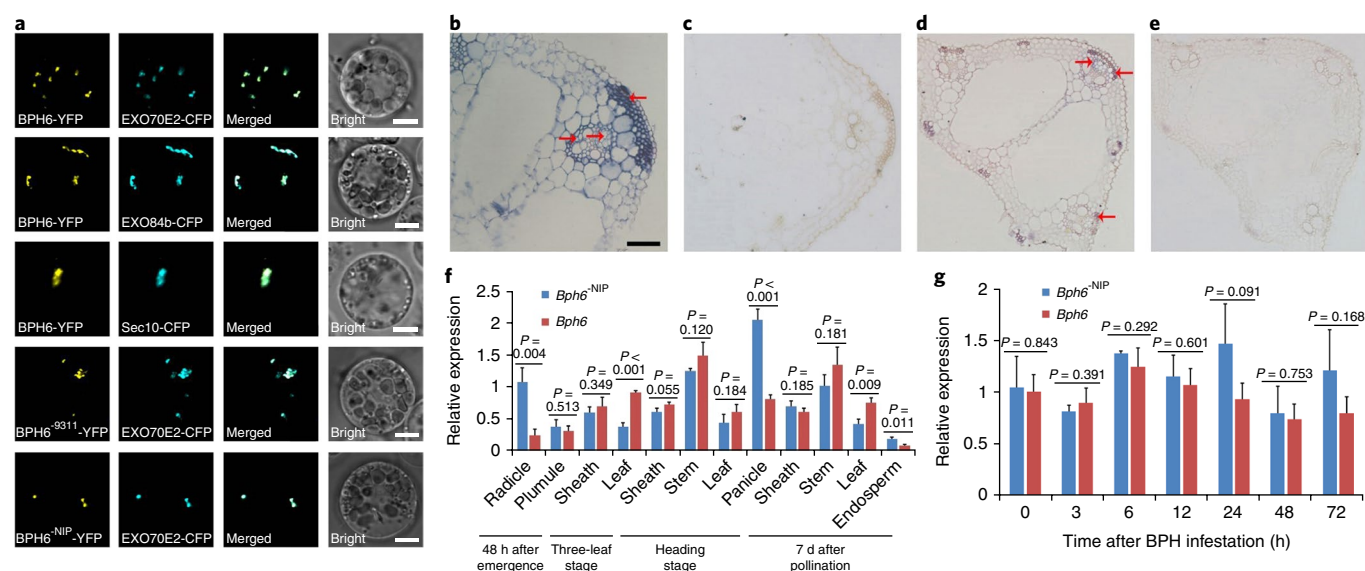


Fig. 2 | Molecular characterization of *Bph6*. **a**, Colocalization of BPH6 and allelic proteins with exocyst subunits EXO70E2, EXO84B and SEC10 in rice protoplasts. YFP-tagged BPH6, BPH6^{-NIP} and BPH6⁻⁹³¹¹ were coexpressed with exocyst subunits EXO70E2, EXO84B and SEC10. Overlapping fluorescence signals show that BPH6 localizes to the exocyst. Bright-field images are shown on the right. Scale bars, 5 μ m. **b–e**, Representative images for in situ hybridization of *Bph6* mRNA in leaf sheaths and leaf cross-sections of NIL plants ($n = 3$ independent experiments with each pooled with 5 individual images). Hybridization with an antisense probe, showing relatively strong signals in sclerenchyma cells, vascular bundles and companion cells in leaf sheaths (**b**) and leaves (**d**) (red arrows), and negative controls using a sense probe (**c,e**). Scale bars, 50 μ m. **f**, Quantification of *Bph6* expression in various organs at the indicated developmental stages. Rice *TBP* was used as reference control. **g**, Quantification of time-dependent expression of *Bph6* in plants infested by BPH. Rice *TBP* was used as a reference control. In **f,g**, data are means \pm s.d.; $n = 3$ independent experiments. *P* values were derived by one-way ANOVA.

in plant–pathogen interactions^{21–23}. Because BPH6 colocalized with exocyst subunits, we tested the possibility that BPH6 interacted with them. We found that BPH6 interacted with OsEXO70E1 (a homolog of EXO70E2 in *Arabidopsis thaliana* (AtEXO70E2) in rice), but not with other exocyst subunit proteins (OsSEC3, OsSEC5, OsSEC6, OsSEC8, OsSEC10, OsSEC15 and OsEXO84), in yeast two-hybrid assays (Fig. 3a and Supplementary Fig. 9). In vivo coimmunoprecipitation (co-IP) assays further confirmed that BPH6 interacted with OsEXO70E1 (Fig. 3b).

The exocyst complex is mainly associated with Golgi-to-plasma-membrane (PM) trafficking, and it participates in various biological processes that require delivery of cytosolic compounds to the PM or to the plant's extracellular environment²¹. We therefore examined the possibility that *Bph6* affects secretion to the cell surface. We first coexpressed OsEXO70E1-YFP and PLC2-CFP (a PM marker protein) with BPH6 or with an empty vector in leaves of *Nicotiana benthamiana*. After 2 d, OsEXO70E1-YFP signals outside the PM (Fig. 3c, small fluorescent punctate structures indicated by the arrows) were detected and measured. A significant difference in the intensity of the OsEXO70E1 fluorescence signal outside the PM (as a proportion of the intensities inside and outside the PM) was observed between cells that coexpressed OsEXO70E1 and BPH6 (4.98%) and others that expressed OsEXO70E1 alone (3.63%) (Fig. 3d). We then tested whether BPH6 could influence release of cytosolic proteins to the cell surface. YFP-tagged rice *S*-adenosylmethionine synthetase 2 (OsSAMS2), a homolog of AtSAMS2 that is delivered to the apoplast and is present in the cell wall proteome²⁰, was selected as a marker. Cells that coexpressed OsSAMS2 and BPH6 generated stronger fluorescence signals outside their PM than cells expressing OsSAMS2 alone (Fig. 3c,d). Collectively these results suggested that *Bph6* could enhance exocytosis.

We further suppressed expression of *OsExo70E1* in Nip-*Bph6*-NIL plants using RNAi targeting *OsExo70E1* expression (hereafter referred to as *OsExo70E1*-RNAi transgenic plants) (Supplementary

Fig. 10a) and evaluated the BPH resistance of the *OsExo70E1*-RNAi transgenic plants. Segregation of resistance was detected in independent T₁ progenies (Fig. 3e). BPH insects that fed on the *OsExo70E1*-RNAi transgenic lines, in which the expression of *OsExo70E1* was suppressed (Supplementary Fig. 10b), excreted much more honeydew and gained much more weight than those that fed on Nip-*Bph6*-NIL plants (Supplementary Fig. 10c,d). Thus, knocking down *OsExo70E1* expression clearly decreased the resistance of Nip-*Bph6*-NIL plants to BPH insects. These results strongly indicate that OsEXO70E1 has a role in *Bph6*-mediated resistance.

***Bph6* has a role in cell wall development in plants infested by BPH.**

The findings that BPH6 protein is localized to the exocyst, interacts with OsEXO70E1 and participates in functions of the exocyst complex prompted us to check expression levels of the exocyst-subunit-encoding genes *Sec3a*, *Sec5*, *Sec6*, *Sec8*, *Sec10* and *Exo70E1* in rice plants before and after BPH feeding. Real-time PCR analysis showed that expression levels of the genes of interest differed between the 9311-*Bph6*-NIL and 9311 plants after BPH feeding for 6 h (Fig. 4a). Generally, their expression was suppressed in 9311 plants but was unchanged or enhanced in 9311-*Bph6*-NIL plants (Fig. 4a), suggesting that exocyst activity is inhibited in susceptible rice but remains normal in *Bph6*-expressing plants infested with BPH. The exocyst-related secretory pathway is essential for building the plant cell wall²⁴. Therefore, we measured cell wall polysaccharides in leaf sheaths of the 9311 and 9311-*Bph6*-NIL plants before and after BPH feeding. The results showed that levels of cell wall components were decreased in 9311 plants, but were unaltered or elevated in 9311-*Bph6*-NIL plants, after BPH feeding (Fig. 4b). We then examined the cell wall monosaccharide composition of leaf sheaths in 9311 and 9311-*Bph6*-NIL plants by GC-MS (gas chromatography–mass spectrometry) analyses. The glucose, xylose and galactose contents were significantly higher in 9311-*Bph6*-NIL plants than in 9311 plants after BPH feeding (Supplementary Table 2).

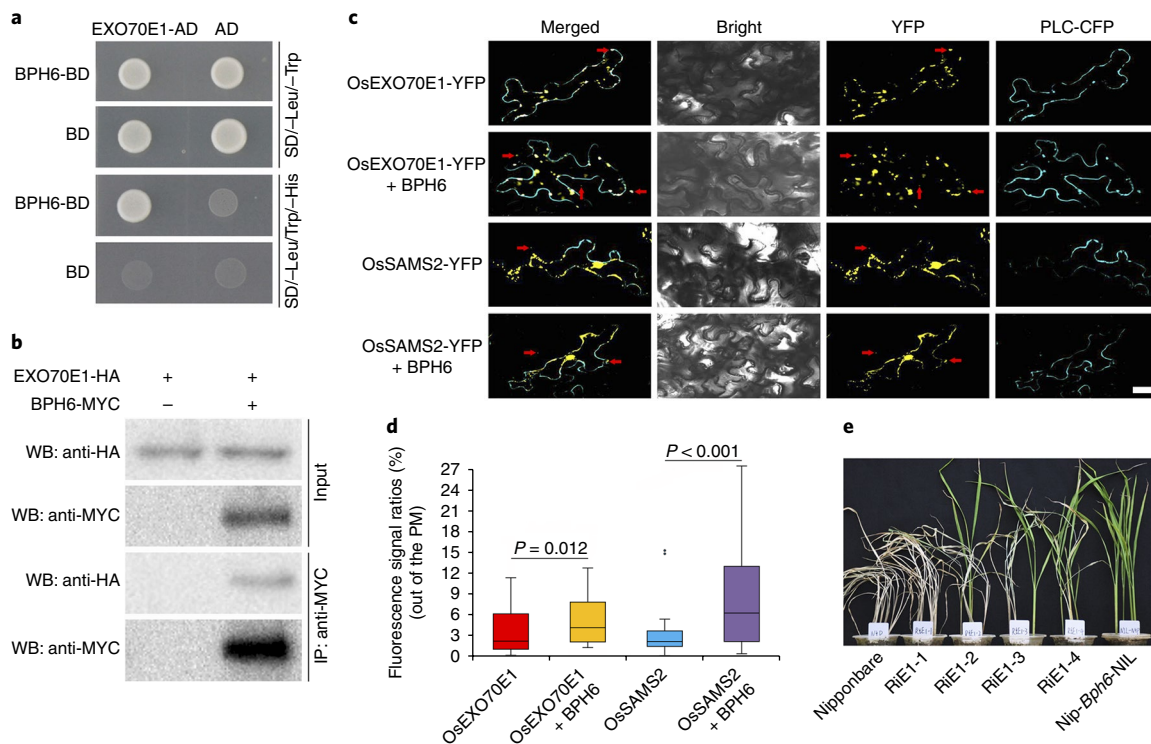


Fig. 3 | Demonstration that BPH6 interacts with exocyst subunit OsEXO70E1. **a,b**, BPH6 interacts with OsEXO70E1 in a yeast two-hybrid assay (**a**) and in rice protoplast co-IP assays (**b**). In **b**, protein that was extracted from rice protoplasts coexpressing the indicated plasmid combinations was analyzed by co-IP. AD, activation domain; BD, DNA-binding domain. $n = 3$ independent experiments. **c,d**, Representative images (**c**) and quantification (**d**) of the presence of the indicated YFP-tagged proteins outside the PM in *N. benthamiana*. (**c**) OsEXO70E1 and OsSAMS2 were detected outside the PM in *N. benthamiana* under the confocal microscope. Confocal micrographs of epidermal cells (treated with 6% NaCl solution for 15 min) of *N. benthamiana* leaves that coexpressed the indicated plasmid combinations. PLC2-CFP was coexpressed as a PM marker. Red arrows indicate signals outside the PM. Scale bar, 20 μm . (**d**) Quantification of ratios of OsEXO70E1-YFP and OsSAMS2-YFP signal intensities outside the PM. Signal intensity distributions of OsEXO70E1-YFP and OsSAMS2-YFP either inside or outside the PM were quantified in the cells. In **c,d**, $n = 3$ (three independent experiments with each pooling 10 individual cells). P values were derived by one-way ANOVA. In the box plots, the center line indicates the median, the box limits are the upper and lower quartiles, and the whiskers mark the range of the data, excluding outliers. **e**, Representative image of *OsExo70E1*-RNAi T₁ progenies and controls after BPH infestation for 7 d ($n = 3$ independent experiments). RIE1-1 to RIE1-4, independent *OsExo70E1*-RNAi T₁ progenies; Nipponbare, susceptible control; Nip-Bph6-NIL, transgenic receptor for *OsExo70E1*-RNAi.

Transmission electron microscopy showed that the cell walls of sclerenchyma tissues, bundle sheaths, sieve tubes and companion cells were significantly thicker in 9311-*Bph6*-NIL than in 9311 plants after BPH infestation for 2 d (Fig. 4c–k and Supplementary Fig. 11). We also observed more callose deposited in the sieve tubes, which prevented the BPH from ingesting phloem sap²⁵, in 9311-*Bph6*-NIL plants than in 9311 plants after BPH infestation (Fig. 4l–n). All of these results suggest that *Bph6* has important roles in maintaining and strengthening the cell walls in leaf sheaths of plants that are infested with BPH insects.

***Bph6* alters phytohormone signaling pathways.** To further investigate the roles of *Bph6* in insect resistance, we analyzed global gene expression profiles during the course of BPH infestation in Nip-*Bph6*-NIL and *Bph6*-RNAi plants, in which *Bph6* expression was knocked down (Supplementary Fig. 5), using Affymetrix GeneChip technology (Supplementary Table 3). The results showed that knocking down *Bph6* expression repressed rice responses to an external stress or stimulus (Supplementary Fig. 12a). More specifically, the expression of genes involved in phytohormone, stress or defense responses, and to oxidation–reduction processes, was significantly weaker in early stages (6 hours after infestation (HAI)), in the RNAi plants than in the Nip-*Bph6*-NIL plants (Supplementary Fig. 12b). At 48 HAI, expression of genes involved in cytokinin

(CK)-regulated processes—such as cytokinesis, cell proliferation and regulation of meristem growth—was also downregulated in the RNAi plants (Supplementary Fig. 12c). Furthermore, genes involved in the salicylic acid (SA), jasmonic acid (JA) and CK biosynthesis and signaling processes were differentially expressed between the Nip-*Bph6*-NIL plants and the RNAi plants at 6 and 48 HAI (Fig. 5a). These findings suggest that *Bph6* expression alters phytohormone signaling pathways, allowing rice to respond rapidly to threats while maintaining growth.

Because phytohormones have pivotal roles in the regulation of plant defense signaling networks²⁶, we quantitatively examined phytohormone profiles in rice plants during BPH infestation (Fig. 5b–d and Supplementary Fig. 13). Generally, phytohormone levels increased more rapidly in the resistant 9311-*Bph6*-NIL plants than in the susceptible 9311 plants in response to BPH infestation. SA, a well-known mediator of BPH resistance in rice¹¹, was induced at relatively high levels in 9311-*Bph6*-NIL plants in early stages (3–6 HAI), whereas no obvious changes were observed in the 9311 plants (Fig. 5b). However, salicylic acid 2-O- β -D-glucoside (SAG), an inactive storage form of SA, was not significantly induced by BPH feeding (Supplementary Fig. 13a). Accumulation of the biologically active form of jasmonates, JA-Ile, which has an important role in plant defenses against wounding and chewing insects²⁷, was significantly and rapidly induced following BPH infestation in

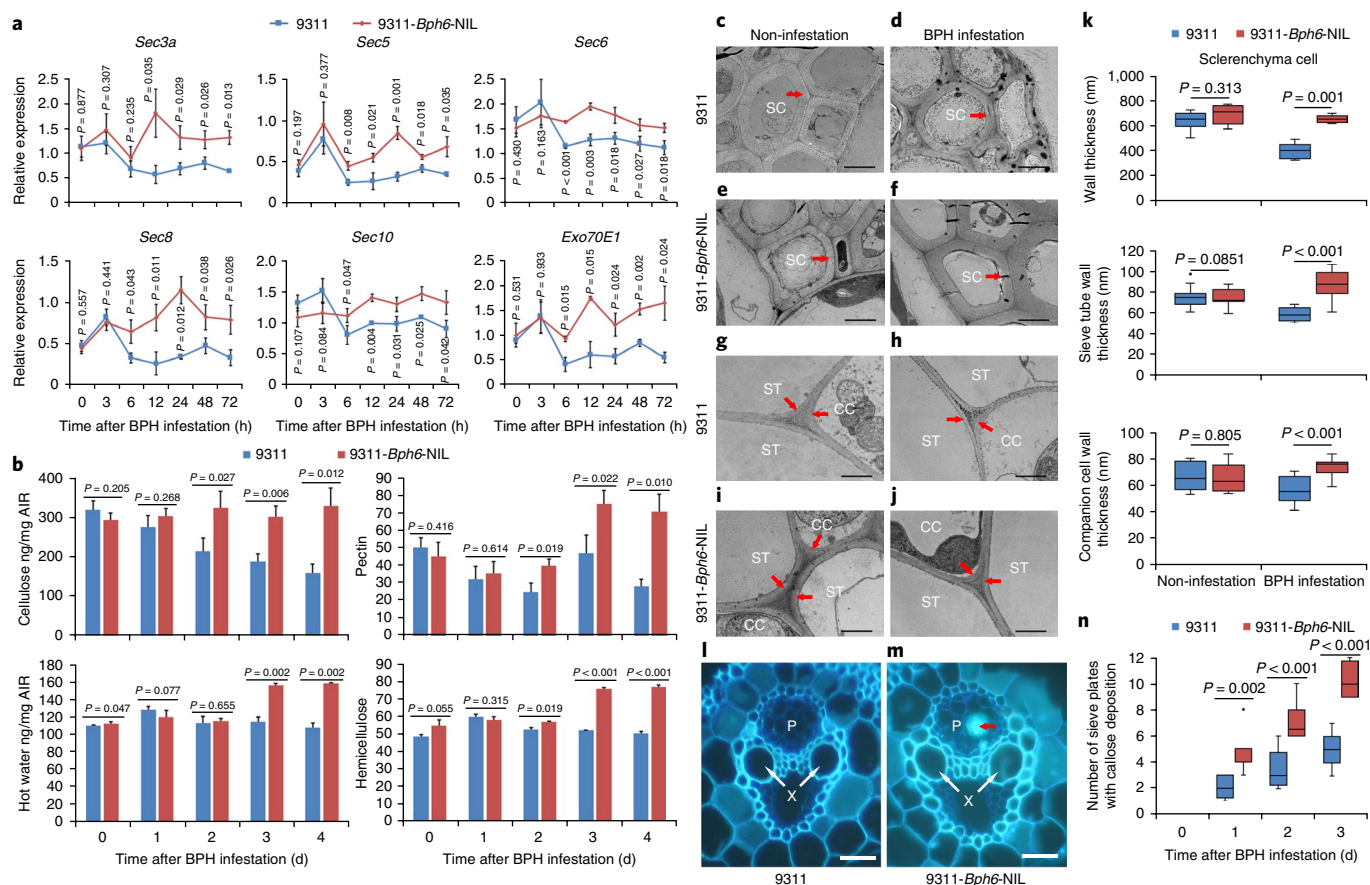


Fig. 4 | Characterization of exocyst gene expression and cell walls in 9311-Bph6-NIL and 9311 plants. **a**, Expression levels of genes encoding exocyst subunits in 9311-Bph6-NIL and 9311 plants infested by BPH. Rice *TBP* was used as a reference control. **b**, Contents of cell wall components in leaf sheaths of 9311-Bph6-NIL and 9311 plants infested by BPH. In **a** and **b**, data are means \pm s.d. of $n=3$ independent experiments. *P* values were derived by one-way ANOVA. **c–k**, Comparison of cell wall thickness in 9311-Bph6-NIL and 9311 plants. Transmission electron micrographs (**c–j**) and quantification of cell wall thickness (**k**) of sclerenchyma cells (**c–f,k**), companion cells and sieve tubes (**g–k**) in 9311 (**c,d,g,h,k**) and 9311-Bph6-NIL (**e,f,i–k**) plants, respectively ($n=3$ independent experiments; data in each pooled from five individual plants and 20 sections). SC, sclerenchyma cell; ST, sieve tube; CC, companion cell. In **k**, sheath sections were used for observation. *P* values were derived by one-way ANOVA. Scale bars, 2 μ m (**c–f**), 0.5 μ m (**g–j**). **l,m**, Representative images showing callose deposition in vascular bundles of 9311 (**l**) and 9311-Bph6-NIL (**m**) plants ($n=10$ independent experiments). The callose is indicated by red arrows. X, xylem; P, phloem. Scale bars, 20 μ m. **n**, Numbers of sieve plates with callose deposition in BPH-infested leaf sheaths ($n=10$ independent experiments; data for each pooled from 50 individual sections). *P* values were derived by one-way ANOVA. In the box plots, the center line denotes the median, box limits are the upper and lower quartiles, and whiskers mark the range of the data, excluding the outliers.

9311-Bph6-NIL plants, and its upregulation lasted longer than in the 9311 plants (Fig. 5c). Most notably, in addition to marked upregulation of the classic defense hormones SA and JA, there was a sharp increase in levels of CKs, especially of the cis-zeatin (cZ) type, in the 9311-Bph6-NIL plants between 12 and 24 HAI as compared to both non-infested controls and 9311 plants (Fig. 5d and Supplementary Fig. 13c–e). The gene expression analyses confirmed the phytohormone regulation patterns (Supplementary Fig. 14). We also quantitatively examined phytohormone levels in *Bph6*-transgenic, Nipponbare, Nip-Bph6-NIL and *Bph6*-RNAi plants after BPH infestation. The results confirmed that levels of SA, JA and cZ-type CKs were higher in *Bph6*-transgenic and Nip-Bph6-NIL plants than in Nipponbare and *Bph6*-RNAi plants (Supplementary Fig. 15).

To further explore the roles of hormones in rice resistance to BPH, we evaluated the BPH survival rate, an indicator of the antibiosis mechanism of plant resistance^{11,14}, on 9311-Bph6-NIL and 9311 plants after treatment with exogenous hormones. Both exogenous SA and methyl jasmonate (MeJA) enhanced resistance, reducing BPH survival rates on 9311-Bph6-NIL and 9311 plants (Fig. 5e and Supplementary Fig. 16a). Thus, contrary to the classic binary defense model of SA and JA, which postulates that they have

opposite roles in defenses against sucking and chewing insects^{28–30} (as well as biotrophic and necrotrophic pathogens³¹), these phytohormones seem to have synergistic effects in rice–BPH interactions. We also tested the effects of treating rice plants with the CKs 6-benzylaminopurine (6-BA), *N*⁶-(Δ^2 -isopentenyl)adenine (iP) and cZ on BPH performance. The survival rates of BPH insects were significantly reduced on the CK-treated 9311-Bph6-NIL plants, suggesting that the CK treatment enhanced resistance (Fig. 5f and Supplementary Fig. 16b,c). In contrast, the BPH survival rate on 9311-Bph6-NIL plants increased when the plants were treated with lovastatin, a CK biosynthesis inhibitor (Supplementary Fig. 16d). However, no such effects of exogenous CKs and lovastatin were observed in the susceptible 9311 plants (Fig. 5f and Supplementary Fig. 16b–d). These findings confirm that CKs have an important role in *Bph6*-mediated resistance. Results of applying the same treatments to *Bph6*-transgenic, Nipponbare, Nip-Bph6-NIL and *Bph6*-RNAi plants confirmed that SA and MeJA enhanced resistance in all of the treated plants, whereas CKs specifically enhanced resistance in *Bph6* plants (Supplementary Fig. 17). These results collectively confirm that *Bph6* mediates resistance by altering the action of CKs, JA and SA.

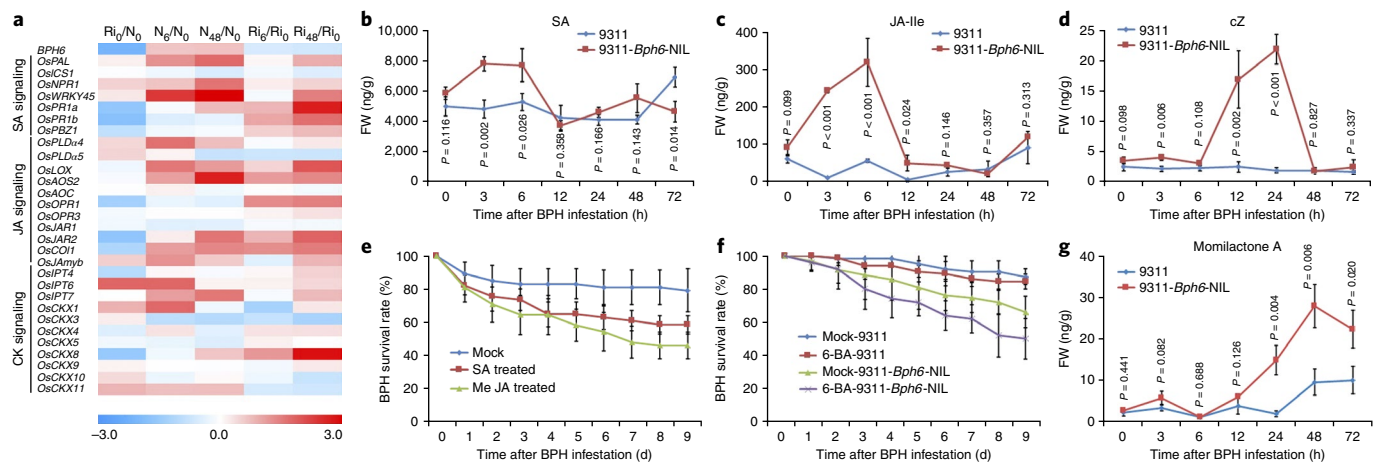


Fig. 5 | Analyses of phytohormones in *Bph6*-carrying plants. **a**, GeneChip analysis of phytohormone-related gene responses to BPH feeding in the Nip-*Bph6*-NIL and *Bph6*-RNAi plants. N_0 , N_6 , N_{48} , Ri_0 , Ri_6 and Ri_{48} , respectively, refer to Nip-*Bph6*-NIL and *Bph6*-RNAi plants sampled at 0, 6 and 48 h after infestation by BPH. **b–d**, Contents of salicylic acid (SA) (**b**), jasmonoyl-L-isoleucine (JA-Ile) (**c**) and cis-zeatin-type cytokinin (cZ) (**d**) in 9311-*Bph6*-NIL and 9311 plants infested by BPH. FW, fresh weight. **e**, Survival rates of BPH insects on SA-, MeJA- and mock-treated 9311-*Bph6*-NIL plants. The survival rate of BPH was significantly lower on 9311-*Bph6*-NIL plants treated with exogenous SA or methyl jasmonate (MeJA) than on mock-treated plants after 4 d of infestation ($P = 0.014$ and 0.035 , respectively). **f**, Survival rates of BPH insects on 6-BA-treated 9311-*Bph6*-NIL and 9311 plants, and on mock-treated controls. Their survival rate was significantly lower on the 6-BA-treated 9311-*Bph6*-NIL plants than on mock-treated 9311-*Bph6*-NIL plants after 7 d of infestation ($P = 0.041$). However, exogenous 6-BA had no detected effect on the 9311 plants. **g**, Momilactone A content in 9311-*Bph6*-NIL and 9311 plants infested by BPH. In **b–g**, data are means \pm s.d. from $n = 3$ independent experiments (**b–d,g**) or $n = 10$ individual plants (**e,f**). P values were derived by one-way ANOVA.

Bph6 and cytokinins positively regulate phytoalexin production.

It has become increasingly apparent recently that CKs have key roles in plant immune systems through various proposed mechanisms, including synthesis of antimicrobial phytoalexins and regulation of defense-associated genes and other defense-related phytohormones^{32–36}. To clarify the mechanism(s) underlying CK-regulated defense against BPH insects in rice, we examined gene expression patterns in CK-treated plants. Expression of *NPR1*, which is essential for SA-induced pathogenesis-related (PR) genes and systemic acquired resistance, was unaffected, whereas expression of *PR1* and *PR5* was slightly induced in CK-treated plants, relative to untreated controls (Supplementary Fig. 18). However, genes involved in biosynthesis of phytoalexins, which have been implicated in chemical defenses against insect herbivores³⁷, were upregulated in the BPH-fed and 6-BA-treated 9311-*Bph6*-NIL plants (Supplementary Figs. 19 and 20a,b). We further examined the effects of BPH feeding and exogenous CK applications on levels of the major rice diterpenoid phytoalexins (momilactones, phytocassanes and oryzalexins) and flavonoid phytoalexins (naringenin and sakuranetin)³⁸. The results showed that BPH feeding induced much stronger increases in momilactone A levels in the 9311-*Bph6*-NIL plants than in the 9311 plants (Fig. 5g). During early stages, it also induced slight rises in naringenin and sakuranetin levels in 9311-*Bph6*-NIL, but not 9311, plants (Supplementary Fig. 21a). 6-BA treatment induced increases in momilactone A levels in the 9311-*Bph6*-NIL plants (Supplementary Fig. 20c). We also measured phytoalexin levels in *Bph6*-transgenic, Nipponbare, Nip-*Bph6*-NIL and *Bph6*-RNAi plants and observed corresponding increases in momilactone A levels, with varying responses in naringenin and sakuranetin levels, after BPH feeding (Supplementary Fig. 21b). Therefore, BPH feeding and exogenous application of CK induced expression of genes involved in phytoalexin biosynthesis and enhanced phytoalexin production in *Bph6*-carrying plants. Furthermore, we analyzed the expression levels of three transcription factors (encoded by *OsTGAP1*, *OsbZIP79* and *OsWRKY76*^{39,40}) involved in regulation of phytoalexin production in rice and found that *OsTGAP1* expression was upregulated and *OsbZIP79* expression was downregulated

in the CK-treated 9311-*Bph6*-NIL plants (Supplementary Fig. 22). The results strongly suggest that CKs are positive regulators of phytoalexin production and *Bph6*-mediated resistance.

***Bph6* confers broad resistance to BPH and WBPH.** Generally, plants may use three resistance mechanisms against insect pests⁴¹—antixenosis, antibiosis and tolerance⁴¹. To probe the mechanisms underlying *Bph6*-controlled resistance, we investigated the responses of BPH insects that were fed on *Bph6*-transgenic, Nipponbare, Nip-*Bph6*-NIL and *Bph6*-RNAi plants. In host-preference experiments, significantly fewer BPH insects settled on *Bph6*-transgenic and Nip-*Bph6*-NIL plants than on Nipponbare and RNAi plants (Fig. 6a and Supplementary Table 4), indicating that there was an antixenotic mechanism. Similarly, fewer BPH eggs were laid on *Bph6*-transgenic and Nip-*Bph6*-NIL plants than on Nipponbare and RNAi plants (Supplementary Fig. 23a and Supplementary Table 4). Electronic penetration graph (EPG) data revealed that the insects ingested phloem for much shorter times on the NIL plants than on the 9311 and Nipponbare plants, showing that insect feeding was inhibited on *Bph6*-carrying plants (Fig. 6b and Supplementary Table 4). Accordingly, the insects excreted less honeydew on *Bph6*-transgenic and Nip-*Bph6*-NIL plants when feeding on them (Fig. 6c and Supplementary Table 4). The BPH survival rate was much lower on the *Bph6*-transgenic and Nip-*Bph6*-NIL plants than on Nipponbare and RNAi plants in a no-choice feeding test (Supplementary Fig. 23b and Supplementary Table 4). All of these observations demonstrate that *Bph6* has both antixenotic and antibiotic effects toward BPH insects.

To assess the resistance spectrum of *Bph6* fully, we evaluated the resistance of 9311-*Bph6*-NIL plants using populations of six BPH biotypes and WBPH. In the tests, the 9311-*Bph6*-NIL plants grew normally, whereas the 9311 plants died after infestation by all of the BPH biotypes (Fig. 6d). The resistance scores of the *Bph6*-carrying plants were 4.11, 2.73, 2.83, 2.80, 2.70 and 3.23 against BPH biotypes 1, 2, 3, P, S and Y, respectively (Fig. 6e). *Bph6* expression also conferred high resistance to WBPH (Fig. 6d,e). However, *Bph6*-carrying plants displayed no resistance to a chewing insect, the

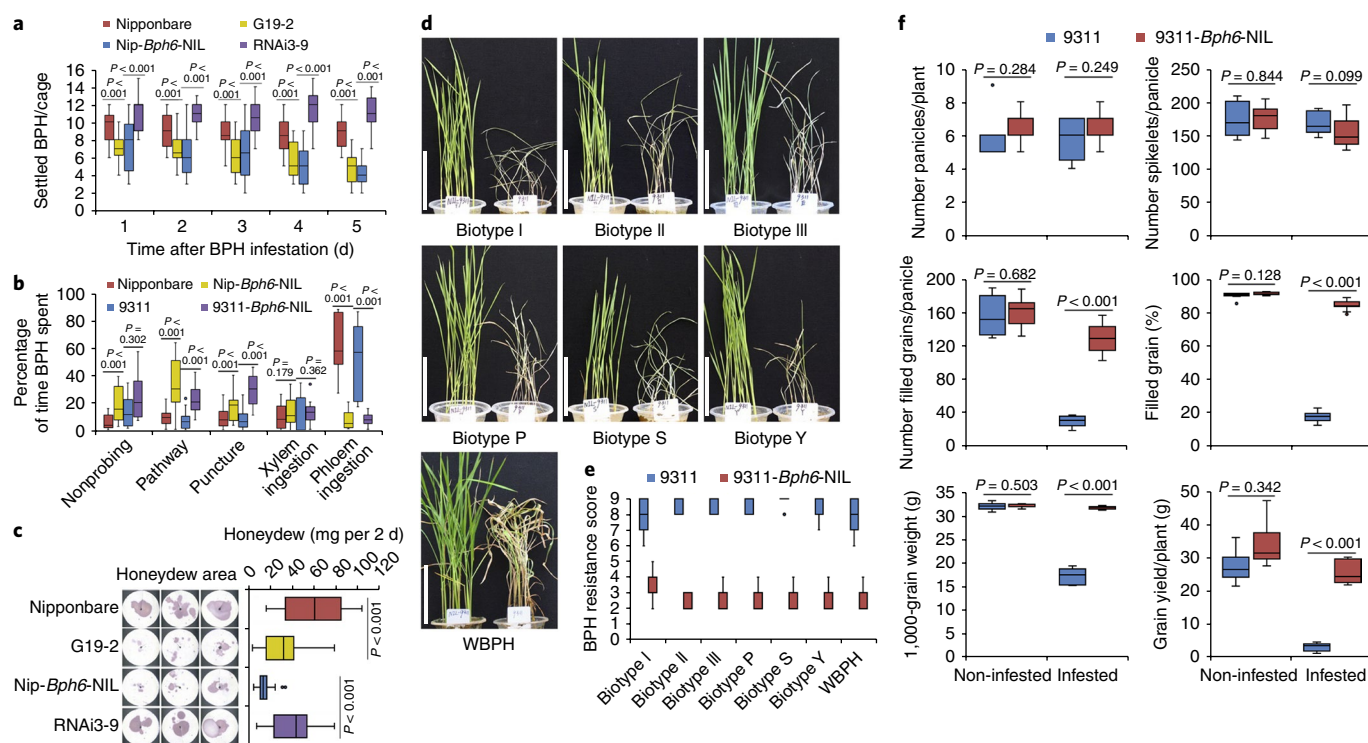


Fig. 6 | Characterization of *Bph6*-mediated resistance. **a**, Settling of BPH insects on Nipponbare, *Bph6*-transgenic (G19-2), Nip-*Bph6*-NIL and *Bph6*-RNAi (RNAi3-9) plants in the host choice test. **b**, Total duration of EPG waveform types indicating durations of activities of BPH insects on Nipponbare, Nip-*Bph6*-NIL, 9311 and 9311-*Bph6*-NIL plants in 8-h recording periods. **c**, Representative images of honeydew (purple-red area in filter paper) excreted by BPH during 2-d feeding on Nipponbare, *Bph6*-transgenic (G19-2), Nip-*Bph6*-NIL and *Bph6*-RNAi (RNAi3-9) plants. Scale bars, 5 mm. In **a–c**, $n = 10$ individual plants. **d**, Photographs illustrating the broad-spectrum resistance conferred by *Bph6* ($n = 3$ independent experiments). Scale bars, 10 cm. **e**, Resistance scores of 9311-*Bph6*-NIL and 9311 seedlings to six BPH biotypes and WBPH. Data were collected 7 d after BPH infestation or 10 d after WBPH infestation. The lower scores indicate higher resistance to the insect, and the higher scores indicate higher susceptibility to the BPH ($n = 3$ independent experiments; data for each pooled from 15 individual plants). **f**, Performance on yield-related traits of 9311-*Bph6*-NIL and 9311 plants observed in the field with and without BPH infestation ($n = 30, 30, 24$ and 22 individual plants for 9311-*Bph6*-NIL and 9311 with and without BPH infestation, respectively; three replicates were analyzed for actual plot yield). In **a–c,e,f**, P values were derived by one-way ANOVA. In each of the box plots, the center line denotes the median, box limits indicate upper and lower quartiles, and whiskers mark the range of the data, excluding outliers.

striped stem borer, or the bacterial blight pathogen *Xanthomonas oryzae* pv. *oryzae* strain PXO145 (Supplementary Fig. 24). These results demonstrate that *Bph6* confers broad-spectrum resistance to different BPH biotypes and to WBPH.

Yield performance of *Bph6*-carrying plants in fields with or without BPH infestation. Cultivated rice is divided into two subspecies, *O. sativa* ssp. *indica* (hereafter referred to as *indica*) and *O. sativa* ssp. *japonica* (hereafter referred to as *japonica*), which widely differ in various genomic, morphologic, agronomic and ecological aspects⁴². 9311 and Nipponbare are typical cultivars of *indica* and *japonica*, respectively. The *Bph6*-NILs in both the 9311 and Nipponbare backgrounds showed high resistance to BPH at the seedling and mature stages (Supplementary Figs. 4 and 25). To further confirm the utility of *Bph6* in breeding programs, we evaluated the resistance and yield performance of 9311-*Bph6*-NIL and 9311 plants under field conditions with and without BPH infestation. In plots that were not infested with BPH, 9311-*Bph6*-NIL and 9311 had similar agronomic traits and grain yields (Fig. 6f and Supplementary Table 5), demonstrating that *Bph6* expression had no adverse effects on rice yields. However, in plots that were heavily infested with BPH, the 9311 plants died and dried, whereas the 9311-*Bph6*-NIL plants showed no clear physiological damage (Supplementary Fig. 26). The percentage of filled grains of BPH-infested 9311 plants was as low as 17.5%, whereas that of BPH-infested 9311-*Bph6*-NIL plants was more than 85%, which is

considered normal. Notably, the BPH infestation heavily reduced 1,000-grain weight and total grain weight and finally caused up to a 90% loss in yield in the 9311 plants. However, the 9311-*Bph6*-NIL plants maintained about 82.2% of their yield (Fig. 5f and Supplementary Table 5). These results demonstrate that, under BPH infestation, *Bph6*-carrying plants are highly resistant to BPH and maintain normal growth and grain yield.

***Bph6* originated in wild rice.** Great genetic diversity, which is essential for plant populations to respond effectively to diverse challenges such as pests and pathogens⁴³, has been commonly observed in cultivated rice and wild species^{44,45}. To explore natural variation of the *Bph6* gene in rice populations, we analyzed its coding sequences from 32 accessions of wild rice and 148 cultivated varieties of various geographic provenance (Supplementary Table 6). High levels of nucleotide variation were observed among the *Bph6* alleles (Supplementary Tables 7 and 8). Average pairwise nucleotide diversity (π) and Watterson's nucleotide diversity estimator (θ_w) over the *Bph6* gene were, respectively, 0.05030 and 0.06407 in wild rice, and 0.07810 and 0.05458 in cultivated rice (Fig. 7a and Supplementary Table 9). Substantial differentiation of the gene was observed between the subspecies *indica* and *japonica*, particularly in the region from 1–1,533 bp that encodes the N terminus of the protein (Supplementary Fig. 1a). However, the sequence diversity of *Bph6* was much lower within *indica* and *japonica* ($\pi = 0.02235$ and $\pi = 0.00807$, respectively) (Fig. 7a and Supplementary Table 9). We

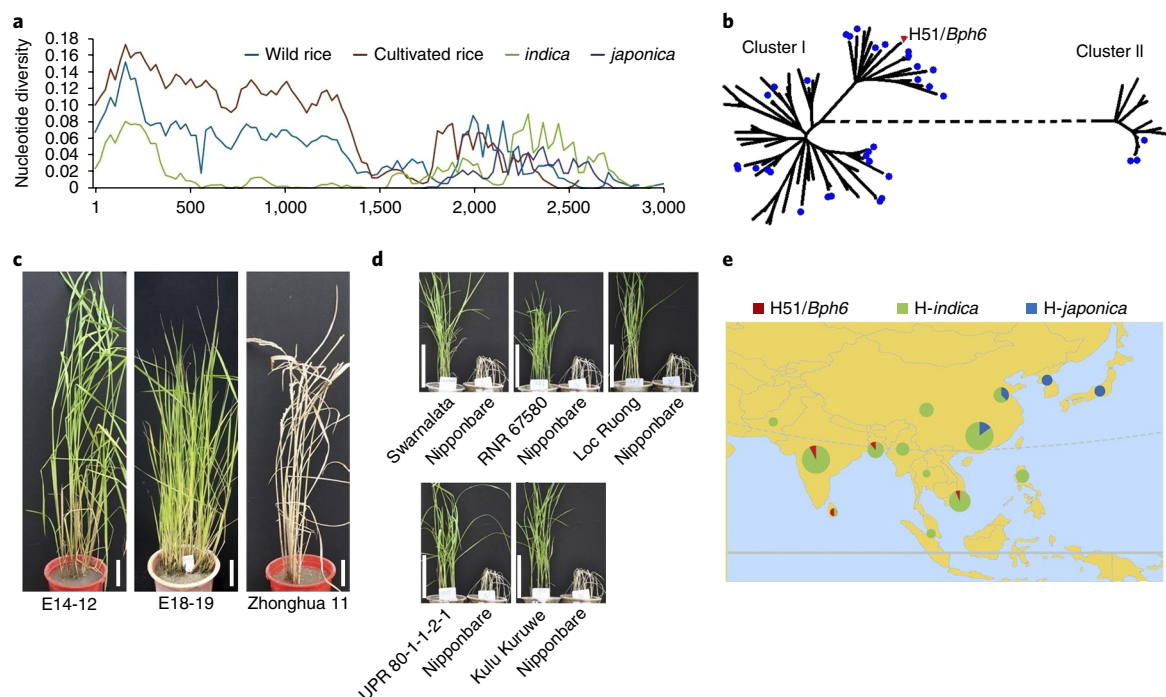


Fig. 7 | Evolution of *Bph6* alleles in rice. **a**, Sliding-window analysis of the nucleotide diversity (π) in the *Bph6* coding region in the indicated rice populations. Values were assigned to the nucleotide at the midpoint of each 25-bp window. The parameter of difference per site (y axis) is plotted against nucleotide position (x axis). **b**, Phylogenetic tree based on haplotypes of *Bph6* alleles in 180 germplasm samples, revealing two major clusters, I and II, which consist mainly of alleles from the *indica* and *japonica* varieties, respectively. H51 (red triangle) is a resistant *Bph6* allele haplotype. Blue circles indicate haplotypes from wild rice. **c**, Representative images for resistance evaluation of accessions of *O. rufipogon* (E14-12) and *O. nivara* (E18-19) carrying *Bph6* at the maturation stage. **d**, Resistance evaluation of five cultivars carrying *Bph6* at the seedling stage. In **c,d**, $n = 3$ independent experiments. Scale bars, 10 cm. **e**, Geographic distribution of *Bph6* haplotypes H51, H-*indica* and H-*japonica* in tropical and temperate regions of Asia. Relative frequencies of the haplotypes in the growing regions of the 148 examined cultivars in each location are represented by the areas of the colored sectors of the pie chart. The size of the pie chart is proportional to the number of varieties. The resistant haplotype H51 (resistant *Bph6* allele, red) is patchily distributed in tropical Asia. Haplotypes that have evolved in *japonica* are distributed in temperate regions. H-*indica* (reseda) represents haplotypes (except H51) in cluster I; H-*japonica* (blue) represents haplotypes in cluster II. The map has been previously described⁴⁷.

identified a total of 80 haplotypes in *Bph6* alleles (Supplementary Table 6) and 45 in the *indica* subspecies, with nine major haplotypes (H9, H19, H22, H23, H51, H52, H53, H54 and H55) scattered evenly in isolation, indicating the gene's heterogeneous nature. Two major haplotypes (H73 and H76) and six others were found in the *japonica* subspecies. The variation in wild rice covers the range observed in cultivated rice (Fig. 7a).

Construction of a phylogenetic tree of *Bph6* haplotypes revealed two major clusters (Fig. 7b), designated cluster I and cluster II, that comprised mainly alleles from *indica* and *japonica*, respectively, confirming the differentiation in *Bph6* alleles between the two subspecies. The highly BPH-resistant allele of *Bph6* is in the haplotype H51, which was present in five tested cultivars (including Swarnalata) and in one accession of each of two species of wild rice (*Oryza rufipogon* and *Oryza nivara*), all of which show resistance to BPH and WBPH (Fig. 7c,d, Supplementary Figs. 1a and 27, and Supplementary Table 10).

Discussion

Secretory pathways play important roles in defense against pathogens by delivering cytosolic compounds that reinforce cell walls, depositing callose and/or releasing antimicrobial compounds²¹. Recently, the evolutionarily conserved exocyst complex, which is involved in the tethering step in the secretory pathways, has emerged as an important battleground in plant–pathogen interaction^{21–23}. Here we isolated *Bph6*, a gene in rice involved in resistance to BPH and WBPH. *Bph6* encodes a novel protein that localizes

to the exocyst and interacts with exocyst subunit OsEXO70E1. Suppression of *OsExo70E1* gene expression decreased resistance of *Bph6*-NIL plants, indicating that *OsExo70E1* participates in *Bph6*-mediated resistance. Our data show that *Bph6* expression enhances release of protein outside the PM. *Bph6* functions in the maintenance and reinforcement of cell walls in rice plants that are infested by BPH. The finding that BPH6 associated with the exocyst complex, and thus with Golgi-to-PM trafficking, paves new avenues to advance understanding of the molecular mechanisms governing plant–insect interactions. Our results also showed that a coordinated CK, SA and JA signaling pathway is activated in *Bph6*-carrying plants after BPH infestation. A notable finding is that CKs function as positive regulators in *Bph6*-mediated resistance. *Bph6* conferred broad resistance to BPH and WBPH, which enabled rice to grow normally under conditions of planthopper infestation, and in the absence of planthoppers *Bph6* carriers showed no yield penalty as *Bph6* expression had no adverse effects on agronomic traits. Thus, *Bph6* expression could clearly be highly beneficial in efforts to control rice planthoppers without other inputs or environmental damage.

Insect herbivores are believed to impose natural selection pressures that favor resistant plant genotypes while driving the evolutionary diversification of plant species⁴⁶. We propose that the resistant *Bph6* allele arose in the wild rice species *O. rufipogon* and *O. nivara* following a host shift of BPH from *Leersia* to *Oryza*, which putatively occurred 0.25 million years ago⁴. After domestication of rice, natural variations in *Bph6* alleles further accumulated mainly

through acquisition of mutations and the major haplotypes formed in *indica* and *japonica*. Although BPH is a rice pest in both tropical and temperate regions, the insects only remain active year round in tropical areas. Thus, constant exposure of rice plants in these areas to planthopper insects presumably promoted enrichment of the resistant haplotype H51 in cultivated rice in these areas. Furthermore, we found that wild rice accessions and cultivated varieties carrying the resistant haplotype H51 are patchily distributed in tropical Asia (Fig. 7e and Supplementary Table 6). In much of this region (for example, in large tracts of India), rice is the staple food, there is a long history of rice cultivation and the selected landraces presumably included resistant alleles. In contrast, two major haplotypes (H73 and H76) evolved in *japonica* and are distributed in temperate areas (Fig. 7e). The resistant *Bph6* allele that arose in wild rice and was retained in cultivars in tropical regions should be very valuable for the development of planthopper-resistant rice varieties and the control of insect pests.

Methods

Methods, including statements of data availability and any associated accession codes and references, are available at <https://doi.org/10.1038/s41588-018-0039-6>.

Received: 8 November 2016; Accepted: 11 December 2017;
Published online: 22 January 2018

References

- Grist, D. H. & Lever, R. J. *Pests of Rice* (Longmans, Green and Co, London, 1969).
- Cheng, X., Zhu, L. & He, G. Towards understanding of molecular interactions between rice and the brown planthopper. *Mol. Plant* **6**, 621–634 (2013).
- Sogawa, K. The rice brown planthopper: feeding physiology and host plant interactions. *Annu. Rev. Entomol.* **27**, 49–73 (1982).
- Sezer, M. & Butlin, R. K. The genetic basis of host plant adaptation in the brown planthopper (*Nilaparvata lugens*). *Heredity* **80**, 499–508 (1998).
- Dyck, V. A. & Thomas, B. in *Brown Planthopper: Threat to Rice Production in Asia* 3–20 (International Rice Research Institute, Manila, Philippines, 1979).
- Catindig, J. L. A. et al. in *Planthoppers: New Threats to the Sustainability of Intensive Rice Production Systems in Asia* 191–220 (International Rice Research Institute, Manila, Philippines, 2009).
- Matsumura, M. et al. in *Planthoppers: New Threats to the Sustainability of Intensive Rice Production Systems in Asia* 233–244 (International Rice Research Institute, Manila, Philippines, 2009).
- Pathak, M. D., Cheng, C. H. & Fortuno, M. E. Resistance to *Nephotettix impicticeps* and *Nilaparvata lugens* in varieties of rice. *Nature* **223**, 502–504 (1969).
- Athwal, D. S., Pathak, M. D., Bacalangco, E. & Pura, C. D. Genetics of resistance to brown planthoppers and green leaf hoppers in *Oryza sativa* L. *Crop Sci.* **11**, 747–750 (1971).
- Ling, Y. & Weilin, Z. Genetic and biochemical mechanisms of rice resistance to planthopper. *Plant Cell Rep.* **35**, 1559–1572 (2016).
- Du, B. et al. Identification and characterization of *Bph14*, a gene conferring resistance to brown planthopper in rice. *Proc. Natl. Acad. Sci. USA* **106**, 22163–22168 (2009).
- Tamura, Y. et al. Map-based cloning and characterization of a brown planthopper resistance gene *BPH26* from *Oryza sativa* L. ssp. *indica* cultivar ADR52. *Sci. Rep.* **4**, 5872 (2014).
- Cheng, X. et al. A rice lectin receptor-like kinase that is involved in innate immune responses also contributes to seed germination. *Plant J.* **76**, 687–698 (2013).
- Liu, Y. et al. A gene cluster encoding lectin receptor kinases confers broad-spectrum and durable insect resistance in rice. *Nat. Biotechnol.* **33**, 301–305 (2015).
- Wang, Y. et al. Map-based cloning and characterization of BPH29, a B3-domain-containing recessive gene conferring brown planthopper resistance in rice. *J. Exp. Bot.* **66**, 6035–6045 (2015).
- Zhao, Y. et al. Allelic diversity in an NLR gene *BPH9* enables rice to combat planthopper variation. *Proc. Natl. Acad. Sci. USA* **113**, 12850–12855 (2016).
- Ren, J. et al. *Bph32*, a novel gene encoding an unknown SCR domain-containing protein, confers resistance against the brown planthopper in rice. *Sci. Rep.* **6**, 37645 (2016).
- Kabir, M. A. & Khush, G. S. Genetic analysis of resistance to brown planthopper resistance gene in rice. *Euphytica* **107**, 23–28 (1988).
- Qiu, Y., Guo, J., Jing, S., Zhu, L. & He, G. High-resolution mapping of the brown planthopper resistance gene *Bph6* in rice and characterizing its resistance in the 9311 and Nipponbare near-isogenic backgrounds. *Theor. Appl. Genet.* **121**, 1601–1611 (2010).
- Wang, J. et al. EXPO, an exocyst-positive organelle distinct from multivesicular endosomes and autophagosomes, mediates cytosol-to-cell-wall exocytosis in *Arabidopsis* and tobacco cells. *Plant Cell* **22**, 4009–4030 (2010).
- Zárský, V., Kulich, I., Fendrych, M. & Pečenková, T. Exocyst complexes multiple functions in plant cells secretory pathways. *Curr. Opin. Plant Biol.* **16**, 726–733 (2013).
- Fujisaki, K. et al. Rice EXO70 interacts with a fungal effector, AVR-Pii, and is required for AVR-Pii-triggered immunity. *Plant J.* **83**, 875–887 (2015).
- Zhao, T. et al. A truncated NLR protein, TIR-NBS2, is required for activated defense responses in the exo70B1 mutant. *PLoS Genet.* **11**, e1004945 (2015).
- Kim, S. J. & Brandizzi, F. The plant secretory pathway: an essential factory for building the plant cell wall. *Plant Cell Physiol.* **55**, 687–693 (2014).
- Hao, P. et al. Herbivore-induced callose deposition on the sieve plates of rice: an important mechanism for host resistance. *Plant Physiol.* **146**, 1810–1820 (2008).
- Pieterse, C. M. J., Van der Does, D., Zamioudis, C., Leon-Reyes, A. & Van Wees, S. C. M. Hormonal modulation of plant immunity. *Annu. Rev. Cell Dev. Biol.* **28**, 489–521 (2012).
- McConn, M., Creelman, R. A., Bell, E., Mullet, J. E. & Browne, J. Jasmonate is essential for insect defense in *Arabidopsis*. *Proc. Natl. Acad. Sci. USA* **94**, 5473–5477 (1997).
- Van der Does, D. et al. Salicylic acid suppresses jasmonic acid signaling downstream of SCFCOII-JAZ by targeting GCC promoter motifs via transcription factor ORA59. *Plant Cell* **25**, 744–761 (2013).
- Zhou, G. et al. Silencing *OsHI-LOX* makes rice more susceptible to chewing herbivores but enhances resistance to a phloem feeder. *Plant J.* **60**, 638–648 (2009).
- Guo, H. M., Li, H. C., Zhou, S. R., Xue, H. W. & Miao, X. X. Cis-12-oxo-phytodienoic acid stimulates rice defense response to a piercing-sucking insect. *Mol. Plant* **7**, 1683–1692 (2014).
- Howe, G. A. & Jander, G. Plant immunity to insect herbivores. *Annu. Rev. Plant Biol.* **59**, 41–66 (2008).
- Naseem, M., Wölfling, M. & Dandekar, T. Cytokinins for immunity beyond growth, galls and green islands. *Trends Plant Sci.* **19**, 481–484 (2014).
- Grosskinsky, D. K. et al. Cytokinins mediate resistance against *Pseudomonas syringae* in tobacco through increased antimicrobial phytoalexin synthesis independent of salicylic acid signaling. *Plant Physiol.* **157**, 815–830 (2011).
- Jiang, C. J. et al. Cytokinins act synergistically with salicylic acid to activate defense gene expression in rice. *Mol. Plant Microbe Interact.* **26**, 287–296 (2013).
- Argueso, C. T. et al. Two-component elements mediate interactions between cytokinin and salicylic acid in plant immunity. *PLoS Genet.* **8**, e1002448 (2012).
- Naseem, M., Kaldorf, M. & Dandekar, T. The nexus between growth and defense signaling: auxin and cytokinin modulate plant immune response pathways. *J. Exp. Bot.* **66**, 4885–4896 (2015).
- Hart, S. V., Kogan, M. & Paxton, J. D. Effect of soybean phytoalexins on the herbivorous insects Mexican bean beetle and soybean looper. *J. Chem. Ecol.* **9**, 657–672 (1983).
- Yamane, H. Biosynthesis of phytoalexins and regulatory mechanisms of it in rice. *Biosci. Biotechnol. Biochem.* **77**, 1141–1148 (2013).
- Ahuja, I., Kissen, R. & Bones, A. M. Phytoalexins in defense against pathogens. *Trends Plant Sci.* **17**, 73–90 (2012).
- Miyamoto, K. et al. Overexpression of the bZIP transcription factor OsbZIP79 suppresses the production of diterpenoid phytoalexin in rice cells. *J. Plant Physiol.* **173**, 19–27 (2015).
- Painter, R. H. in *Insect Resistance in Crop Plants* 23–83 (Macmillan, New York, 1951).
- Sang, T. & Ge, S. Understanding rice domestication and implications for cultivar improvement. *Curr. Opin. Plant Biol.* **16**, 139–146 (2013).
- Fisher, M. C. et al. Emerging fungal threats to animal, plant and ecosystem health. *Nature* **484**, 186–194 (2012).
- Huang, X. et al. A map of rice genome variation reveals the origin of cultivated rice. *Nature* **490**, 497–501 (2012).
- Xu, X. et al. Resequencing 50 accessions of cultivated and wild rice yields markers for identifying agronomically important genes. *Nat. Biotechnol.* **30**, 105–111 (2011).
- Agrawal, A. A., Hastings, A. P., Johnson, M. T., Maron, J. L. & Salminen, J. P. Insect herbivores drive real-time ecological and evolutionary change in plant populations. *Science* **338**, 113–116 (2012).
- Yan, W. et al. Natural variation in *Ghd7.1* plays an important role in grain yield and adaptation in rice. *Cell Res.* **23**, 969–971 (2013).

Acknowledgements

We thank Q. Qian (China National Rice Research Institute), L. Han (Chinese Academy of Agricultural Sciences), L. Yan (Jiangxi Academy of Agricultural Sciences) and D. Pan (Guangdong Academy of Agricultural Sciences) for kindly providing rice germplasm, S. Wang (Huazhong Agricultural University) for kindly providing the rice disease pathogen PXO145, Y. Lin (Huazhong Agricultural University) for kindly providing the striped stem borer insects, D. Zeng (China National Rice Research Institute) for kindly providing the WBPH insects, Y. Liu for suggestions for the experiments, and Q. Zhang, R. He and J. Blackwell for edits and suggestions. This work was supported by grants from the National Natural Science Foundation of China (31230060 and 31630063, both to G.H.), the National Program on Research and Development of Transgenic Plants (2016ZX08009-003-001 to G.H.) and the National Key Research and Development Program (2016YFD0100600 and 2016YFD0100900, both to G.H.).

Author contributions

G.H. conceived and supervised the project; G.H. and J.G. designed the experiments; J.G. performed most of the experiments; C.X., Y.Z., D.W., B.D., X.W., Y.O., X.L., W.W., Y.Q.,

S.J., B.C., X.S., H.W., Y.M., Y.W., L.H., S.S., L.Z., X.X., R.C. and Y.F. performed some of the experiments; and J.G., C.X., D.W., B.D., Y.Z. and G.H. analyzed data and wrote the manuscript.

Competing interests

The authors declare no competing financial interests.

Additional information

Supplementary information accompanies this paper at <https://doi.org/10.1038/s41588-018-0039-6>.

Reprints and permissions information is available at www.nature.com/reprints.

Correspondence and requests for materials should be addressed to B.D. or G.H.

Publisher's note: Springer Nature remains neutral with regard to jurisdictional claims in published maps and institutional affiliations.

Methods

Plant and insect materials. Seeds of the rice cultivar Swarnalata, which has been previously described⁴⁸, were kindly provided by the International Rice Research Institute. 9311-*Bph6*-NIL and Nip-*Bph6*-NIL are near-isogenic lines that carry *Bph6* from Swarnalata in genetic backgrounds of the insect-susceptible model varieties 9311 and Nipponbare (which are *indica* and *japonica* subspecies, respectively). The *Bph6*-NIL lines were generated by repeated backcrossing to the recurrent parent, as well as marker-aided selection, to eliminate introgression of non-target DNA regions, as previously described⁴⁹.

BPH insects are maintained in the authors' laboratory. Biotypes 1, 2, 3, P and Y were separately maintained on plants of rice varieties TN1, Mudgo, ASD7, P09 (which carries the BPH-resistance gene *Bph9*) and YHY15 (which carries *Bph15*), as previously described⁴⁹. Population S insects were collected from rice fields in Wuhan, China, and maintained on TN1 plants for 3 years.

WBPH insects were collected from rice fields in Hangzhou, China, and maintained on susceptible cultivar TN1 in the laboratory. The larvae of the striped stem borer (SSB; *Chilo suppressalis* Walker) were obtained from a colony maintained in the laboratory. The bacterial blight pathogen *X. oryzae* pv. *oryzae* strain PXO145 was cultured on potato dextrose agar medium in the laboratory¹³.

Evaluation of BPH and WBPH resistance of rice. The rice resistance scores were obtained by a progeny test⁵⁰. BPH and WBPH resistance of rice populations at the seedling stage was evaluated by using at least three replicates of each cultivar or line as previously described^{50,51}. Briefly, sets of about 60 seeds from each population were randomly sown in separate plastic boxes in three 26-cm-long rows, with 2.5 cm between rows, or 20 seeds harvested from an individual plant were sown in a 10-cm-in-diameter plastic cup. At the third-leaf stage, each seedling was infested with ten BPH or WBPH nymphs (second- to third-instar). When all of the susceptible 9311 or Nipponbare control plants had died (scored as 9), each seedling of the other cultivars or lines was given a score of 0, 1, 3, 5, 7 or 9, as previously described^{50,51} and calculated. To evaluate resistance at the maturing stage, each of the rice plants was grown in a 20-cm-in-diameter plastic bucket and infested with 100 mature BPH insects at the heading stage. About a month later, the plants were scored as susceptible (dead) or resistant (alive).

Performance of BPH and SSB insects, and inoculation with pathogen on rice plants. BPH insect performance on rice plants was evaluated using host choice, fecundity, nymph survival rate, honeydew excretion and EPG assays, as previously described^{11,14,25}. Seeds of each line were sown in a plastic cup (10 cm in diameter), and seedlings at the four-leaf stage were infested with BPH. All of the experiments were repeated ten times. In the host-choice test, seedlings in the cup were covered with a light-transmitting mesh, and ten BPH nymphs per plant were released. The number of insects on each plant were recorded at 1, 2, 3, 4 and 5 d after release. In the BPH fecundity assay, each plant was infested with two couples of BPH adults. After 7 d, the adults were removed, and the numbers of eggs laid on leaf sheath were counted under the microscope. To study BPH nymph survival on rice, second-instar BPH nymphs were released (ten insects per plant), and then the cups were covered with a light-transmitting mesh. The nymphs on each plant were counted 8 d after release. To measure honeydew excretion, a filter paper (4 cm in diameter) was placed on the base of a rice plant, and the plant was covered by an inverted transparent plastic cup. Ten third-instar nymphs that had previously been starved for 2 h were placed in the chamber. After 2 d, the filter papers were collected and treated with a solution of 0.1% ninhydrin in acetone. After drying for 30 min at 60°C, the honeydew spots appeared as violet or purple stains due to their amino acid content. To weigh the honeydew, a Parafilm sachet was attached to the leaf sheath of each seedling. A female BPH within 1 d after emergence was then enclosed in the sachet. After 2 d, the insect was removed, and the sachet was weighed. For EPG assays of BPH insects feeding on rice plants, a female BPH within 1 d after emergence was attached with gold wire on its dorsum and placed on the leaf sheath. The test continued for 8 h. Data were acquired at 100-Hz sample frequency, stored on a computer's hard disc and simultaneously displayed on a screen. The EPG waveforms indicative of BPH feeding behavior patterns have been previously described²⁵.

SSB insect performance on rice plants was evaluated using larval survival rate and growth mass, as previously described⁵². To assess the resistance to bacterial blight, rice plants at the tillering stage were inoculated with PXO145 by leaf clipping as previously described¹³.

High-resolution mapping of *Bph6*. Previously, we used the flanking markers RM16994 and RM17008 to screen 4,300 BC₃F₂ plants, obtain 41 recombinants and map *Bph6* to the region between markers Y9 and Y19¹⁹. Additional DNA markers were designed based on the published genomic sequences of Nipponbare and 9311 in the GeneBank database, and these were used to analyze the recombinants and delimit the *Bph6* gene to the 18.1-kb region flanked by the markers H and Y9 in our current study.

***Bph6* complementation and knockdown.** To construct plasmids for the complementation test, coding sequence (CDS) fragments of *Gene1* and *Gene2* were amplified from Swarnalata by using gene-specific primers (Supplementary

Table 11), and the PCR products were inserted into the binary vector pCXUN⁵³ (after the A-addition procedure) to generate complementation constructs, which were designated GENE1 and GENE2, respectively. After verification by DNA sequencing, these constructs were transformed into Nipponbare using the *Agrobacterium*-mediated method. The *Bph6*-RNAi construct was developed by amplifying a 498-bp fragment of *Gene1* cDNA using primers Ripri1 and Ripri2 (Supplementary Table 11) and inserting it into the binary vector pCXUN as previously described⁵⁴. This construct was transformed into Nip-*Bph6*-NIL plants to generate the RNAi plants.

Total rice genomic DNA was isolated from leaves of T₀ transgenic plants as previously described⁴⁰ and subjected to Southern blot analysis using a North2South Complete Biotin Random Prime Labeling and Detection Kit (Thermo Fisher Scientific). Briefly, 4 µg DNA samples were digested with *DraI* restriction enzyme, fractionated by electrophoresis, transferred to nylon membrane and allowed to hybridize with a 728-bp biotinylated *hpt* II probe.

To identify the T-DNA insertion site, a genome walker system was used. The genomic DNA libraries were prepared by digesting the T₀ progeny plant DNA with four blunt-ended enzymes and then ligated to specific adapters following the Universal Genome Walker Kit user manual (CLONTECH). The fragments resulting from the PCR reactions performed on the Genome Walker libraries were sequenced, and 5' sequences upstream of the LB (left border) region were analyzed. Sequences of the primers are listed in Supplementary Table 11.

The *OsExo70E1*-RNAi construct was developed by amplifying a 486-bp fragment of *OsExo70E1* using primers Ri70E1-1 and Ri70E1-2 (Supplementary Table 11) and inserting it into the binary vector pCXUN⁵⁴. This construct was transformed into Nip-*Bph6*-NIL plants to generate the *OsExo70E1*-RNAi plants.

RNA isolation, quantitative RT-PCR analysis and RACE. Total RNAs were isolated from rice plants using TRIzol reagent (Invitrogen), according to the manufacturer's instructions, and then converted into first-strand cDNA (PrimeScrip RT Reagent Kit with gDNA Eraser, Takara, RR047Q). Expression of *Bph6* and other genes involved in BPH feeding responses was analyzed by quantitative RT-PCR using a CFX96 Real-Time System (Bio-Rad). Sequences of the primers used are listed in Supplementary Table 11.

For 5' RACE, we conducted the first round of amplification according to the protocol provided with the Advantage 2 PCR Kit (CLONTECH) using the primer 5RACE1R and the UPM adaptor primer from the kit. For the second round, the PCR product from the first round was diluted 50-fold, and 1 µl of this solution was used as the template. The amplification was conducted using the nest primer 5RACE2R together with the adaptor primer NUPM provided in the kit. The 3' RACE protocol was essentially the same, except that primers 3RACE1F (with UPM) and 3RACE2F (with NUPM) were used in the first and second amplification rounds, respectively. Sequences of the primers are listed in Supplementary Table 11.

Subcellular localization analysis. The *Bph6*, *Bph6*⁻⁹³¹¹ (9311 allele of *Bph6*) and *Bph6*^{-NIP} (Nipponbare allele of *Bph6*) coding sequences, amplified by PCR using the primers *Bph6*-GFP and *Bph6*^{-NIP}-GFP (Supplementary Table 11), were cloned downstream of a maize (*Zea mays*) ubiquitin-1 promoter, in frame with XFP (GFP or YFP) in the binary vector pCambia1300, yielding, respectively, constructs named BPH6-XFP, BPH6⁻⁹³¹¹-YFP and BPH6^{-NIP}-YFP. Full-length cDNAs encoding other exocyst subunits (*AtSec10* and *AtExo84b*) were amplified from *Arabidopsis* Columbia-0 leaf tissue cDNAs with the primer sets listed in Supplementary Table 11. The expression constructs were coexpressed into rice protoplasts according to previously described protocols⁴⁵. The resulting XFP fluorescence was visualized under a confocal laser-scanning microscope (FV1000, Olympus).

The standard organelle markers were as follows: bZIP63⁵³ for the nucleus, mRFP-SYP61²⁰ for the TGN/EE, EXO70E2²⁰ for the exocyst, CD3-953 for the endoplasmic reticulum (ER), CD3-961 for the cis-Golgi, and CD3-969⁵⁶ for the tonoplast. We developed the EXO70E2-CFP-expressing constructs, and the corresponding amplified fragments (encoding EXO70E2)²⁰ were cloned into the pGWB17 vector with cyan fluorescent tags at the C terminus.

RNA in situ hybridization. Freshly collected rice leaf sheaths and leaves were fixed in 4% paraformaldehyde in PBS, pH 7.0, for 30 min, and then in a fresh paraformaldehyde solution at 4°C overnight. The samples were subsequently washed in PBS, dehydrated in a graded ethanol series and embedded in Paraplast Plus (Sigma-Aldrich) at 58–60°C. We cut ~12-µm-thick microtome sections and mounted them on RNase-free glass slides.

To prepare a *Bph6* probe, we used a pair of primers, insitu-F and insitu-R (Supplementary Table 11), to amplify a unique 173-bp sequence of Swarnalata *Bph6* (and alleles) from a cDNA clone. The fragment was then inserted into the pTA-2 vector (Toyobo) for RNA transcription. The sense and antisense RNA probes were produced by T7 and T3 RNA polymerase labeled with digoxigenin (Roche). RNA in situ hybridization and immunological detection followed previously described protocols⁵⁷.

Yeast two-hybrid assay. The Matchmaker GAL4 yeast two-hybrid system 3 (CLONTECH) was used for yeast two-hybrid assays. *Bph6* was amplified and

cloned into the pGBKT7 vector using the primers shown in Supplementary Table 11. Genes encoding exocyst subunits (*OsSec3*, *OsSec5*, *OsSec6*, *OsSec8*, *OsSec10*, *OsSec15*, *OsExo70E1* and *OsExo84*) were amplified from Nipponbare tissue cDNAs with the primer sets listed in Supplementary Table 11 and cloned into the pGADT7 vector. These plasmids were cotransformed into yeast strain AH109 with the pGBKT7-*Bph6* construct, and the transformants were simultaneously grown on synthetic dropout (SD) medium lacking leucine and tryptophan or on SD medium (containing an appropriate concentration of 3-amino-1,2,4-triazole (3AT)) lacking leucine, tryptophan and histidine.

Immunoblot analysis and in vivo co-immunoprecipitation assays. For immunoblot analysis, total protein from rice leaf sheaths was extracted in protein extraction buffer (50 mM Tris-HCl pH 7.5, 150 mM NaCl, 10% glycerol, 0.1% NP-40, 1 mM PMSF and plant protease inhibitor cocktail (Roche)). Equal amounts of total protein were analyzed by SDS-PAGE and detected by immunoblotting using anti-actin (Abbkine, Catalog: A01050-2) or anti-BPH6 antibodies. The relative intensities of the protein bands were quantified by Image J software. The anti-BPH6 antibody was prepared by expressing amino acids 1–140 of BPH6 (cloned into pET28a) in *Escherichia coli* strain BL21. The expressed recombinant proteins were harvested and injected into a rabbit (Quan Biotech Corp, Wuhan, China).

In vivo Co-IP assays were carried out by transient protein expression in rice protoplasts. Hemagglutinin (HA)-tagged EXO70E1 and MYC-tagged BPH6 or MYC-empty constructs were coexpressed in rice protoplasts, extracted in the buffer described above, immunoprecipitated with an anti-MYC antibody (MBL, M192-3), then detected by the anti-HA (MBL, catalog: M180) and anti-Myc (MBL, catalog: M047), respectively.

Transient expression in *N. benthamiana* and quantification of fluorescence signals. The *Agrobacterium* strain GV3101 containing expression vectors was grown overnight at 28°C. Cells were resuspended and incubated in induction medium (containing 10 mM MES pH 5.6, 10 mM MgCl₂ and 150 μM actosyringone) at room temperature for 2 h before infiltration by direct injection. *Agrobacterium* suspensions used in co-infiltration experiments were mixed to the desired final OD₆₀₀ values and then injected into the leaves of 5- to 6-week-old *N. benthamiana* plants with a needleless syringe. Two days after infiltration, the plant leaves were subjected to osmotic treatment with 6% NaCl solution for 15 min and then observed with a confocal microscope (FV1000, Olympus).

To compare proportions of fluorescence signals outside the PM of cells in *N. benthamiana* leaves that were transiently expressing different combinations of constructs, we first measured the raw integrated signal density divided by the areas of regions of interest (ROIs) outside and inside the PM of 30 cells of leaves expressing each tested combination, then calculated average values of the intensity ratio (as percentages of the intensity outside the PM). Three replicates were used for each combination of constructs.

Transmission electron microscopy. Fresh leaf sheaths were fixed with 3% glutaraldehyde in PBS, pH 7.2, for 4 h at room temperature. The samples were subsequently washed in PBS, postfixed with 1% osmium tetroxide, dehydrated in a graded ethanol series and embedded in Spurr's resin (Sigma-Aldrich, EM0300). Samples were sectioned using an ultramicrotome. For transmission electron microscopy, ultrathin sections were post-stained with uranyl acetate for 10 min, followed by lead citrate for 2 min. The sections were then observed with a JEM-1400 plus transmission electron microscope (Japan).

Cell wall analysis. The alcohol-insoluble residue (AIR) of cell walls from leaf sheaths from 9311-*Bph6*-NIL and 9311 plants infested by BPH for different times were prepared as previously described⁵⁸. The AIR was de-starched by treatment with α-amylase (0.75 U/mg, Sigma) in 10 mM Tris-maleate buffer (pH 6.9) overnight. After removing the solubilized starch by centrifugation, the hot-water-soluble pectin and hemicellulose fractions were extracted with hot water, 50 mM EDTA (pH 6.8) and 17.5% sodium hydroxide containing 0.04% sodium borohydride, followed by heating in a boiling water bath for 10 min, respectively. The hemicellulose fractions were neutralized with acetic acid, dialyzed against water at 4°C for 1 d and lyophilized. The residual precipitate was washed with water and ethanol, then collected as the cellulose fraction. The total sugar content of the fractions was determined by the phenol-sulfuric acid method⁵⁹ using glucose as a calibration standard. The crystalline cellulose content was measured by using a modified method as described by Updegraff⁶⁰.

The de-starched AIR was sequentially fractionated, and the analysis of uronic acid and monosaccharide composition was performed by GC-MS (Thermo Fisher Scientific) as previously described⁵⁸.

Callose deposition in rice tissue. To observe callose deposition, rice seedlings at the three-leaf stage were each infested with ten BPH insects. Their leaf sheaths were then fixed in FAA solution (50% ethanol, 5% acetic acid and 3.7% formaldehyde) at 4°C overnight, dehydrated and embedded in Paraplast Plus (Sigma-Aldrich) at 58–60°C. Sections, ~10 μm thick, of the samples were taken, mounted on glass slides, stained with 0.1% aniline blue in 0.1 M K₂PHO₄ for 5 min, and then examined under a fluorescence microscope (BX51, Olympus).

The callose deposition in each examined plant was scored by counting the number of sieve plates with a bright callose ring. At least 400 sections were examined per sample, and the results were expressed as the number recorded per 50 sections, as previously described²⁷.

Microarray analysis. Nip-*Bph6*-NIL and *Bph6*-RNAi (RNAi3-9) rice seedlings were grown in the Plant Growth Chamber (CONVIRON PGC2000, Canada), and each was infested with ten third-instar BPH nymphs at the four-leaf stage and sampled at 0 (non-infested control), 6 and 48 h after BPH infestation. All treatments, each with three biological replicates, were terminated at the same time. Total RNA was isolated from the sampled leaf sheaths using TRIzol reagent (Invitrogen) according to the manufacturer's instructions. The transcriptomic profiles were then explored using standard Affymetrix instruments, protocols and software (obtained from Shanghai Bio Corp.). The acquired data were then analyzed using the 'limma' software package to detect differentially expressed genes (DEGs), with fold-change ≥2.0 and probability criteria <0.01 or <0.05 (ref. ⁶¹). The experiments were repeated three times.

Measurement of phytohormones and phytoalexins. Seeds were sown in plastic cups (10 cm in diameter) and grown in the Plant Growth Chamber (CONVIRON PGC2000, Canada) under programmed conditions (relative humidity, 80% from 0:00 to 19:30 and 75% from 19:30 to 0:00; light intensity, level 3; and temperature: 0:00–5:30, 25°C, 5:30–8:30, 27°C, 8:30–11:30, 30°C, 11:30–15:30, 32°C, 15:30–17:00, 30°C, 17:00–19:30, 28°C, 19:30–0:00, 27°C). For BPH treatment, plants of the treated groups were infested with ten BPH nymphs (ten per plant) at the selected time points (3, 6, 12, 24, 48 and 72 h to the end of experiments). Control groups were maintained in parallel but without BPH infestation⁶². At the end of the treatments, leaf sheaths were collected from the rice plants. All treatments were repeated three times. Phytohormones and phytoalexins were extracted from rice leaf sheaths and analyzed by ultrafast liquid chromatography with electrospray ionization and tandem mass spectrometry (UFLC-ESI-MS) as previously described⁶³. Three replicates of each frozen sample were ground to a fine power in liquid nitrogen and extracted with a methanol:water:acetic acid (80:19:1, vol/vol/vol) solution supplemented with internal standards. After centrifugation, the supernatant was filtered through a nylon membrane with 0.22-μm pores. The filtrate was dried and re-dissolved in methanol for quantification of phytohormones and phytoalexins. SAG was extracted, purified and analyzed as previously described⁶⁴.

Phytohormone treatment of rice plants. SA (1 mM), MeJA (25 μM), 6-BA (50 μM), iP (10 μM), cZ (10 nM) and lovastatin (50 μM) were sprayed individually on leaf sheaths of *Bph6*-NIL, *Bph6*-transgenic and WT rice plants at the three-leaf stage. To study nymph survival on seedlings, ten third-instar nymphs were placed on each plant 6 h later. The cup was covered with light-transmitting mesh, and the number of nymphs on each plant was counted 9 d after infestation. The experiments were repeated ten times. The leaf sheaths were collected 6 h later for quantitative RT-PCR analysis and phytoalexin measurement. The experiments were repeated three times.

Sequence analyses of *Bph6* alleles in rice collections. *Bph6* alleles from 148 cultivars and 32 accessions of wild rice species were sequenced (Supplementary Table 6). The genomic sequences corresponding to the transcribed regions of *Bph6* and *Bph6*^{NIP} were amplified with four primer sets (Bph6-1, Bph6-2, Bph6^{NIP}-1 and Bph6^{NIP}-2; Supplementary Table 11). Numbers of polymorphic sites (S) and haplotypes (H), the average pairwise differences per base pair between sequences (π) and Watterson's estimator (θ_w) were calculated using DnaSP (version 5)⁶⁵. A phylogenetic tree of *Bph6* haplotypes was generated from multiple open-reading frame sequence alignments by CLUSTAL X. The phylogeny of sequences was inferred by the neighbor-joining (NJ) method and conducted with MEGA (version 6.0)⁶⁶. Bootstrap analyses were performed with 1,000 replicates.

Yield performance test in field. To investigate effects of *Bph6* on yield performance and resistance in field conditions, we grew 9311 and *Bph6*-NIL plants in Wuhan, China, under a standard field management regime for the region. The experiment was laid out in a randomized block design with three replications. Seedlings, 30 d old, of all experimental materials were transplanted in the field with 16.7 cm spacing between plants within each line and 26.7 cm between rows. The 'severe BPH populations' plot received BPH at the heading stage. Briefly, we infested ~10,000 mature BPH insects in each plot. At harvest, the middle six to ten plants in the central row of each plot were sampled for analysis. The following seven quantitative traits of these plants were then assessed and recorded: heading date (in days), plant height (in cm), panicles per plant (in number), spikelets per panicle (in number), grains per panicle (in number), percentage of filled grain, 1,000-grain weight (in grams) and grain yield per plant (in grams)⁶⁷.

Statistical analyses. Statistical analysis of all the data was performed using one-way ANOVA in Microsoft Excel. The traits evaluated in the field are summarized in Supplementary Table 5.

URLs. National Center for Biotechnology Information (NCBI), <https://www.ncbi.nlm.nih.gov>; Rice Information System (RIS), <http://rise2.genomics.org.cn/page/rice/index.jsp>; Michigan State University (MSU) Rice Genome Annotation Project, <http://rice.plantbiology.msu.edu/>; The *Arabidopsis* Information Resource (TAIR), <http://www.arabidopsis.org/>.

Life Sciences Reporting Summary. Further information on experimental design is available in the Life Sciences Reporting Summary.

Data availability. The NCBI accessions for genome and cDNA sequence of the *Bph6* allele from Swarnalata are [KX818198](#) and [KX818197](#), respectively. The microarray data have been deposited in the Gene Expression Omnibus (GEO) under accession code [GSE86379](#).

References

48. Qiu, Y. F. et al. Identification of antibiosis and tolerance in rice varieties carrying brown planthopper resistance genes. *Entomol. Exp. Appl.* **141**, 224–231 (2011).
49. Jing, S. et al. Development and use of EST-SSR markers for assessing genetic diversity in the brown planthopper (*Nilaparvata lugens* Stål). *Bull. Entomol. Res.* **102**, 113–122 (2012).
50. Huang, Z., He, G. C., Shu, L. H., Li, X. H. & Zhang, Q. F. Identification and mapping of two brown planthopper resistance genes in rice. *Theor. Appl. Genet.* **102**, 929–934 (2001).
51. Heinrichs, E., Medrano, F. & Rapusas, H. in *Genetic Evaluation of Insect Resistance in Rice* (International Rice Research Institute, Manila, Philippines, 1985).
52. Yang, Z., Chen, H., Tang, W., Hua, H. & Lin, Y. Development and characterization of transgenic rice expressing two *Bacillus thuringiensis* genes. *Pest Manag. Sci.* **67**, 414–422 (2011).
53. Walter, M. et al. Visualization of protein interactions in living plant cells using bimolecular fluorescence complementation. *Plant J.* **40**, 428–438 (2004).
54. Chen, S., Songkumarn, P., Liu, J. & Wang, G. L. A versatile zero background T-vector system for gene cloning and functional genomics. *Plant Physiol.* **150**, 1111–1121 (2009).
55. Zhang, Y. et al. A highly efficient rice green tissue protoplast system for transient gene expression and studying light- and chloroplast-related processes. *Plant Methods* **7**, 30 (2011).
56. Nelson, B. K., Cai, X. & Nebenführ, A. A multicolored set of in vivo organelle markers for colocalization studies in *Arabidopsis* and other plants. *Plant J.* **51**, 1126–1136 (2007).
57. Weng, Q. M., Huang, Z., Wang, X. L., Zhu, L. L. & He, G. C. In situ localization of proteinase inhibitor mRNA in rice plant challenged with brown planthopper. *Chin. Sci. Bull.* **48**, 979–982 (2003).
58. Pettolino, F. A., Walsh, C., Fincher, G. B. & Bacic, A. Determining the polysaccharide composition of plant cell walls. *Nat. Protoc.* **7**, 1590–1607 (2012).
59. Dubois, M., Gilles, K. A., Hamilton, J. K., Robers, P. A. & Smith, F. Colorimetric method for determination of sugars and related substances. *Anal. Chem.* **28**, 350–356 (1956).
60. Updegraff, D. M. Semimicro determination of cellulose in biological materials. *Anal. Biochem.* **32**, 420–424 (1969).
61. Smyth, G. K. Linear models and empirical Bayes methods for assessing differential expression in microarray experiments. *Stat. Appl. Genet. Mol. Biol.* **3**, e3 (2004).
62. Liu, C. et al. Revealing different systems responses to brown planthopper infestation for pest-susceptible and resistant rice plants with the combined metabolomic and gene expression analysis. *J. Proteome Res.* **9**, 6774–6785 (2010).
63. Liu, H., Li, X., Xiao, J. & Wang, S. A convenient method for simultaneous quantification of multiple phytohormones and metabolites: application in study of rice–bacterium interaction. *Plant Methods* **8**, 2 (2012).
64. Yuan, H. M., Liu, W. C. & Lu, Y. T. CATALASE2 coordinates SA-mediated repression of both auxin accumulation and JA biosynthesis in plant defenses. *Cell Host Microbe* **21**, 143–155 (2017).
65. Librado, P. & Rozas, J. DnaSPv5: a software for comprehensive analysis of DNA polymorphism data. *Bioinformatics* **25**, 1451–1452 (2009).
66. Tamura, K., Stecher, G., Peterson, D., Filipowski, A. & Kumar, S. MEGA6: molecular evolutionary genetics analysis version 6.0. *Mol. Biol. Evol.* **30**, 2725–2729 (2013).
67. You, A. et al. Identification of quantitative trait loci across recombinant inbred lines and testcross populations for traits of agronomic importance in rice. *Genetics* **172**, 1287–1300 (2006).